Hindawi
Journal of Function Spaces
Volume 2023, Article ID 7918713, 14 pages
https://doi.org/10.1155/2023/7918713

Research Article

Barycentric Interpolation Collocation Method for Solving Fractional Linear Fredholm-Volterra Integro-Differential Equation

Jin Li,[1,2] **Kaiyan Zhao**,[1] **and Xiaoning Su**[1]

[1]*College of Science, North China University of Science and Technology, Tangshan 063210, China*
[2]*Hebei Key Laboratory of Data Science and Application, North China University of Science and Technology, Tangshan 063210, China*

Correspondence should be addressed to Kaiyan Zhao; zhaokaiyan@stu.ncst.edu.cn

Received 20 November 2022; Revised 11 September 2023; Accepted 15 September 2023; Published 3 October 2023

Academic Editor: Selma Gulyaz

In this article, barycentric interpolation collocation method (BICM) is presented to solve the fractional linear Fredholm-Volterra integro-differential equation (FVIDE). Firstly, the fractional order term of equation is transformed into the Riemann integral with Caputo definition, and this integral term is approximated by the Gauss quadrature formula. Secondly, the barycentric interpolation basis function is used to approximate the unknown function, and the matrix equation of BICM is obtained. Finally, several numerical examples are given to solve one-dimensional differential equation.

1. Introduction

The concept of the fractional calculus dates back to 1695. Fractional differential equations, as a generalization of integer differential equations, are suitable for describing materials and processes with genetic and memory properties. Compared with integer order model, fractional order model can simulate dynamic system and natural physical phenomena more accurately. Fractional models are widely used in many fields, such as biological engineering [1–3], mechanics [4, 5], physics [6], electromagnetism [7, 8], viscoelastic system [9, 10], and heat conduction engineering [11]. Moreover, many researchers have proposed some efficient methods to investigate the existence and uniqueness of the solutions of fractional differential equations [12–18].

Lately, many researchers insinuated some standards to classify fractional differential operators. The notion of offering a guideline in a field was satisfactory enough, although the list of items that were suggested presented a limitation along with the critics brought up that were not academically acceptable. As a result of these criticisms, numerous researchers investigated the list along with their outcomes rejected the index law; in [19], their outcomes invalidated that inclusion of index law in the field. In another research work, the authors did overall investigation of the diffusive function of some kernel [20] and the outcomes they presented suggested that only operators with nonindex law properties can have crossover diffusive behaviors. However, Caputo and Fabrizio proved that the suggested index law was not right or it was a restriction to the field, and in their turn, they offered a list of items to be followed [21]. Further, they also proved the necessity of nonsingular differential operators along with their applications to nature applications to nature. In [22], the authors presented an optimal control of diffusion using the Atangana–Baleanu fractional differential operator. They proved that the existence of the solution with Atangana–Baleanu derivatives was obtained when the fractional order $\alpha \in (0, 1)$, and they also mentioned that the existence of the solution with Riemann-Liouville and Caputo was achieved during $\alpha \in (0,0.5)$.

Furthermore, definitions of two well-known fractional derivatives, namely, Riemann-Liouville and Caputo [23], included a singular kernel. However, Caputo and Fabrizio introduced another definition having a nonsingular kernel

and properties can be found in [24]. Another derivatives with nonsingular kernel were suggested in [25] which fundamentally generalized the Caputo and Fabrizio definition [26]. However, Riemann-Liouville fractional derivative be essential in the development of theory of fractional derivatives and integrals. But, this derivative barely able to generate physical interpretation of the initial conditions that are compulsory for the initial value issues containing fractional differential equations and also the boundary value issue both of the issues can be solved with the Caputo definition of fractional derivative for further details, refer [27]. Another difference is that the derivative of a constant is not zero for Riemann-Liouville, but it is equal to zero for Caputo. Additionally, the Riesz fractional derivatives have some shortcomings, such as it relies upon the values of whole interval also not sustaining the Leibniz rule for the product of two functions [28]. Besides, the Caputo fractional definition is easy to calculate and program. So the Caputo derivative is chosen in this manuscript.

In this paper, we mainly solve the FVIDE

$$\begin{aligned} {}_0^C D_t^\alpha y(t) + \int_0^t K_v(t,x)y(x)dx + \int_a^b K_f(t,z)y(z)dz \\ = g(t), 0 \le t \le T, \end{aligned} \tag{1}$$

where $\int_0^t K_v(t,x)y(x)dx$ is the Volterra part, $\int_a^b K_f(t,z)y(z)dz$ is the Fredholm part, ${}_0^C D_t^\alpha y(t)$ is the fractional derivative part, and the fractional derivative is defined as the Caputo definition as follows:

$${}_0^C D_t^\alpha y(t) = \frac{1}{\Gamma(\xi-\alpha)} \int_0^t \frac{\partial^\xi y(\tau)}{\partial \tau^\xi} \frac{d\tau}{(t-\tau)^{\alpha+1-\xi}}, \tag{2}$$

where $\Gamma(\cdot)$ is the Gamma function.

The initial condition of one-dimensional differential equation is given as

$$y(0) = A. \tag{3}$$

In recent years, many methods are proposed to solve fractional differential equations. In [29], the Bell polynomials are introduced to solve fractional differential equations based on matrix and collocation points. In [30], the central difference and Crank-Nicolson method are used to obtain the full discrete scheme of spatial fractional convection-diffusion equation; then, the Richardson extrapolation method is used to further improve the calculation accuracy. In [31, 32], the finite element method is presented to solve fractional convection-diffusion equations. In [33–35], the element free Galerkin method is used to solve fractional differential equations. Compared with other algorithms, BICM has the advantages of high precision, easy programming, and simple formula. Therefore, this method has been applied to solve various equations, such as heat conduction equation [36], generalized Poisson equation [37], fractional differential equation [38], and fractional reaction-diffusion equation [39]. At the same time, the BICM is also utilized to solve some engineering problems, such as the plane elasticity problem [40], the bending problem of elliptic plate [41], and the numerical approximation of Darcy flow [42].

In this article, BICM is introduced to solve FVIDE. In Section 2, we provide relevant definitions of barycentric interpolation. In Sections 3–5, barycentric interpolation basis function is applied to approximate the unknown function, and matrix equations of the fractional derivative part, Volterra part, and Fredholm part are given. In Section 6, we obtain the matrix equation of FVIDE, and initial condition is dealt with by replacement method or additive method. In Section 7, some numerical examples are shown to prove feasibility of the algorithm.

2. Barycentric Interpolation

In this section, we will introduce barycentric interpolation for solving one-dimensional differential equation. First, $n+1$ equidistant nodes or Chebyshev's nodes are chosen as collocation points on the domain, i.e., (t_i), $i = 0, 1, \cdots, n$. The barycentric interpolation function is defined as

$$y_n(t) = \sum_{i=0}^{n} T_i(t) y_i, \tag{4}$$

where $y_i = y_n(t_i)$ and

$$T_i(t) = \frac{w_i/(t-t_i)}{\sum_{k=0}^{n} w_k/(t-t_k)}. \tag{5}$$

According to different definitions of weight functions w_i, barycentric interpolation can be divided into barycentric rational interpolation and barycentric Lagrange interpolation. The weight functions of barycentric Lagrange interpolation are defined as

$$w_i = \frac{1}{\prod_{j=0, j\neq i}^{n} t_i - t_j}, \tag{6}$$

the weight functions of barycentric rational interpolation are defined as

$$\begin{aligned} w_i &= \sum_{s\in D_i} (-1)^s \prod_{k=s, s\neq i}^{s+d} \frac{1}{t_i - t_k}, \\ D_i &= \{s : i-d \le s \le i\}, \end{aligned} \tag{7}$$

where $s \in \{0, 1, \cdots, n-d\}$, the parameter d is integer, and $0 \le d \le n$.

3. Matrix Equation of Fractional Derivative Part

Fractional terms are dealt with by integration by parts; then, we get

$$\begin{aligned} {}_0^C D_t^\alpha y(t) &= \frac{1}{\Gamma(\xi-\alpha)}\int_0^t \frac{\partial^\xi y(\tau)}{\partial\tau^\xi}\frac{d\tau}{(t-\tau)^{\alpha+1-\xi}} \\ &= \frac{1}{\Gamma(\xi+1-\alpha)}\frac{\partial^\xi y(0)}{\partial t^\xi}t^{\xi-\alpha} \\ &\quad + \frac{1}{\Gamma(\xi+1-\alpha)}\int_0^t \frac{\partial^{\xi+1} y(\tau)}{\partial\tau^{\xi+1}}\frac{d\tau}{(t-\tau)^{\alpha-\xi}} \\ &= \Gamma_\alpha^\xi\left[\frac{\partial^\xi y(0)}{\partial t^\xi}t^{\xi-\alpha} + \int_0^t \frac{\partial^{\xi+1} y(\tau)}{\partial\tau^{\xi+1}}\frac{d\tau}{(t-\tau)^{\alpha-\xi}}\right], \end{aligned} \tag{8}$$

where $\Gamma_\alpha^\xi = 1/(\Gamma(\xi+1-\alpha))$.

Substituting equation (4) into equation (8), we obtain

$${}_0^C D_t^\alpha y_n(t) = \Gamma_\alpha^\xi \sum_{i=0}^n \left[T_i^{(\xi)}(0)t^{\xi-\alpha}\right]y_i + \Gamma_\alpha^\xi \sum_{i=0}^n \left[\int_0^t \frac{T_i^{(\xi+1)}(\tau)}{(t-\tau)^{\alpha-\xi}}d\tau\right]y_i, \tag{9}$$

where

$$T_i(\tau) = \frac{w_i/(\tau-\tau_i)}{\sum_{k=0}^n w_k/(\tau-\tau_k)}. \tag{10}$$

Let $t = t_\theta$, formula (9) can be expressed as

$${}_0^C D_{t_\theta}^\alpha y_n(t_\theta) = \Gamma_\alpha^\xi \sum_{i=0}^n \left[T_i^{(\xi)}(0)t_\theta^{\xi-\alpha}\right]y_i + \Gamma_\alpha^\xi \sum_{i=0}^n \left[\int_0^{t_\theta} \frac{T_i^{(\xi+1)}(\tau)}{(t_\theta-\tau)^{\alpha-\xi}}d\tau\right]y_i, \tag{11}$$

where $\theta = 0, 1, \cdots, n$.

Let us write the integral term of the formula (11) as the following form:

$$\begin{aligned} P_{\theta i} = P_i(t_\theta) &= \int_0^{t_\theta} T_i^{(\xi+1)}(\tau)(t_\theta-\tau)^{\xi-\alpha}d\tau, \\ i &= 0, 1, \cdots, n. \end{aligned} \tag{12}$$

Then, we have

$${}_0^C D_{t_\theta}^\alpha y_n(t_\theta) = \Gamma_\alpha^\xi\left\{\sum_{i=0}^n \left[T_i^{(\xi)}(0)t_\theta^{\xi-\alpha}\right] + \sum_{i=0}^n [P_{\theta i}]\right\}y_i. \tag{13}$$

The integral term (12) is calculated using the Gauss quadrature formula with weights $\rho(\tau) = (t_\theta-\tau)^{\xi-\alpha}$; we get

$$P_{\theta i}^G = \sum_{j=1}^m T_i^{(\xi+1)}\left(\tau_j^{\theta,\alpha}\right)A_j^{\theta,\alpha}, \tag{14}$$

where $\tau_j^{\theta,\alpha}$ and $A_j^{\theta,\alpha}$ are the Gauss points and Gauss weights and m is the number of the Gauss points.

Using the Gauss-Legendre quadrature formula, equation (15) is given as

$$P_{\theta i}^{\mathrm{GL}} = \frac{t_\theta}{2}\sum_{j=1}^m f\left(\tau_j^{\theta,l}\right)A_j^{\theta,l}, \tag{15}$$

where $\tau_j^{\theta,l}$ and $A_j^{\theta,l}$ are integral points and integral weights, m is the number of the integral points, $t_\theta/2$ is transformed coefficient, and $f(\tau_j^{\theta,l}) = \rho(\tau_j^{\theta,l})T_i^{(\xi+1)}(\tau_j^{\theta,l})$.

Then, the formula (16) with the Gauss quadrature formula is obtained as

$$\begin{bmatrix} {}_0^C D_{t_0}^\alpha y_n(t_0) \\ \vdots \\ {}_0^C D_{t_n}^\alpha y_n(t_n) \end{bmatrix} = \Gamma_\alpha^\xi\left[T^{\xi,\alpha}\left(I_{n+1}\otimes M_1^{(\xi)}\right) + I_{n+1}\otimes P\right]\begin{bmatrix} y_0 \\ \vdots \\ y_n \end{bmatrix}, \tag{16}$$

where I_{n+1} is the identity matrix and $\otimes$ is the Kronecker product.

Briefly, the formula (16) can be written as

$$D = D^\alpha Y, \tag{17}$$

where

$$D^\alpha = \Gamma_\alpha^\xi\left[T^{\xi,\alpha}\left(I_{n+1}\otimes M_1^{(\xi)}\right) + I_{n+1}\otimes P\right],$$

$$Y = \begin{bmatrix} y_0 \\ \vdots \\ y_n \end{bmatrix},$$

$$D = \begin{bmatrix} {}_0^C D_{t_0}^\alpha y_n(t_0) \\ \vdots \\ {}_0^C D_{t_n}^\alpha y_n(t_n) \end{bmatrix},$$

$$T^{\xi,\alpha} = \begin{bmatrix} t_\theta^{\xi-\alpha} & & & \\ & t_\theta^{\xi-\alpha} & & \\ & & \ddots & \\ & & & t_\theta^{\xi-\alpha} \end{bmatrix}_{N\times N},$$

$$P = \begin{bmatrix} P_{11} & P_{12} & \cdots & P_{1N} \\ P_{21} & P_{22} & \cdots & P_{2N} \\ \vdots & \vdots & \ddots & \vdots \\ P_{N1} & P_{N2} & \cdots & P_{NN} \end{bmatrix}_{N\times N},$$

$$N = n+1,$$

$$P_{11} = \sum_{j=1}^m T_0^{(\xi+1)}\left(\tau_j^{0,\alpha}\right)A_j^{0,\alpha},$$

$$
\begin{aligned}
P_{12} &= \sum_{j=1}^{m} T_1^{(\xi+1)}\left(\tau_j^{0,\alpha}\right) A_j^{0,\alpha},\\
P_{1N} &= \sum_{j=1}^{m} T_n^{(\xi+1)}\left(\tau_j^{0,\alpha}\right) A_j^{0,\alpha},\\
P_{21} &= \sum_{j=1}^{m} T_0^{(\xi+1)}\left(\tau_j^{1,\alpha}\right) A_j^{1,\alpha},\\
P_{22} &= \sum_{j=1}^{m} T_1^{(\xi+1)}\left(\tau_j^{1,\alpha}\right) A_j^{1,\alpha},\\
P_{2N} &= \sum_{i=1}^{m} T_n^{(\xi+1)}\left(\tau_j^{1,\alpha}\right) A_j^{1,\alpha},\\
P_{N1} &= \sum_{j=1}^{m} T_0^{(\xi+1)}\left(\tau_j^{n,\alpha}\right) A_j^{n,\alpha},\\
P_{N2} &= \sum_{j=1}^{m} T_1^{(\xi+1)}(\tau_i^{n,\alpha}) A_j^{n,\alpha},\\
P_{NN} &= \sum_{j=1}^{m} T_n^{(\xi+1)}\left(\tau_j^{n,\alpha}\right) A_j^{n,\alpha}.
\end{aligned} \tag{18}
$$

The relations between differential matrices and basis functions are defined as follows:

$$
M^{(h)} = \left[M_{\theta i}^{(h)}\right]_{N\times N} = \left[T_i^{(h)}(t_\theta)\right]_{N\times N}, \tag{19}
$$

where $N = n + 1$ and

$$
\begin{aligned}
M_{\theta i}^{(1)} &= \begin{cases} \dfrac{w_i/w_\theta}{t_\theta - t_i}, & \theta \neq i, \\ -\sum\limits_{i\neq\theta} M_{\theta i}^{(1)}, & \theta = i, \end{cases}\\
M_{\theta i}^{(\xi)} &= \begin{cases} \xi\left(M_{\theta\theta}^{(\xi-1)} M_{\theta i}^{(1)} - \dfrac{M_{\theta i}^{(\xi-1)}}{t_\theta - t_i}\right), & \theta \neq i, \\ -\sum\limits_{i\neq\theta} M_{\theta i}^{(\xi)}, & \theta = i. \end{cases}
\end{aligned} \tag{20}
$$

Hence, we can get

$$
M_1^{(\xi)} = \begin{bmatrix} -\sum\limits_{i=1}^{n} M_{0i}^{(\xi)} & M_{01}^{(\xi)} & M_{02}^{(\xi)} & \cdots & M_{0n}^{(\xi)} \\ -\sum\limits_{i=1}^{n} M_{0i}^{(\xi)} & M_{01}^{(\xi)} & M_{02}^{(\xi)} & \cdots & M_{0n}^{(\xi)} \\ \vdots & \vdots & \vdots & \ddots & \vdots \\ -\sum\limits_{i=1}^{n} M_{0i}^{(\xi)} & M_{01}^{(\xi)} & M_{02}^{(\xi)} & \cdots & M_{0n}^{(\xi)} \end{bmatrix}_{N\times N}. \tag{21}
$$

4. Matrix Equation of the Volterra Part

The Volterra part is expressed as $V(t)$; equation (22) is shown as follows:

$$
V(t) = \int_0^t K_\nu(t, x) y(x) dx. \tag{22}
$$

Substituting equation (4) into equation (22), we obtain

$$
V_n(t) = \sum_{i=0}^{n} \left[\int_0^t K_\nu(t, x) T_i(x) dx\right] y_i, \tag{23}
$$

where $T_i(x)$ is defined as shown in equation (10).

t is replaced by t_θ of formula (23), and we have

$$
V_n(t_\theta) = \sum_{i=0}^{n} \left[\int_0^{t_\theta} K_\nu(t_\theta, x) T_i(x) dx\right] y_i, \tag{24}
$$

where $\theta = 0, 1, \cdots, n$.

Formula (25) is expressed in the following form:

$$
Q_{\theta i} = Q_i(t_\theta) = \int_0^{t_\theta} K_\nu(t_\theta, x) T_i(x) dx. \tag{25}
$$

Using the Gauss quadrature formula with weights $\beta(x) = K_\nu(t_\theta, x)$, we get

$$
Q_{\theta i}^{G} = \sum_{j=1}^{m} T_i\left(x_j^\theta\right) C_j^\theta, \; i = 0, 1, \cdots, n, \tag{26}
$$

where x_j^θ and C_j^θ are the Gauss points and Gauss weights and m is the number of the Gauss points.

Formula (25) is calculated by the Gauss-Legendre quadrature formula, and we obtain

$$
Q_{\theta i}^{\mathrm{GL}} = \frac{t_\theta}{2} \sum_{j=1}^{m} q\left(x_j^{\theta,l}\right) C_j^{\theta,l}, \tag{27}
$$

where $x_j^{\theta,l}$ and $C_j^{\theta,l}$ are integral points and integral weights, m is the number of the integral points, $t_\theta/2$ is transformed coefficient, and $q(x_j^{\theta,l}) = \beta(x_j^{\theta,l}) T_i^{(\xi+1)}(x_j^{\theta,l})$.

Combining equation (24), equation (25), and equation (26), equation (28) is obtained

$$
V_n(t_\theta) = \sum_{i=0}^{n} \left[Q_{\theta i}^{G}\right] y_i. \tag{28}
$$

Let $V_i = V_n(t_i)$; formula (29) is obtained as follows:

$$
V = QY, \tag{29}
$$

where

$$V = \begin{bmatrix} V_0 \\ \vdots \\ V_n \end{bmatrix},$$

$$Y = \begin{bmatrix} y_0 \\ \vdots \\ y_n \end{bmatrix},$$

$$Q = \begin{bmatrix} Q_{11} & Q_{12} & \cdots & Q_{1N} \\ Q_{21} & Q_{22} & \cdots & Q_{2N} \\ \vdots & \vdots & \ddots & \vdots \\ Q_{N1} & Q_{N2} & \cdots & Q_{NN} \end{bmatrix}_{N\times N}, \tag{30}$$

$$N = n+1, Q_{11} = \sum_{j=1}^{m} T_0\left(x_j^0\right) C_j^0,$$

$$Q_{12} = \sum_{j=1}^{m} T_1\left(x_j^0\right) C_j^0, Q_{1N} = \sum_{j=1}^{m} T_n\left(x_j^0\right) C_j^0,$$

$$Q_{21} = \sum_{j=1}^{m} T_0\left(x_j^1\right) C_j^1, Q_{22} = \sum_{j=1}^{m} T_1\left(x_j^1\right) C_j^1,$$

$$Q_{2N} = \sum_{i=1}^{m} T_n\left(x_j^1\right) C_j^1, Q_{N1} = \sum_{j=1}^{m} T_0\left(x_j^n\right) C_j^n,$$

$$Q_{N2} = \sum_{j=1}^{m} T_1(x_i^n) C_j^n, Q_{NN} = \sum_{j=1}^{m} T_n\left(x_j^n\right) C_j^n.$$

5. Matrix Equation of the Fredholm Part

The Fredholm part is expressed as the following form:

$$I(t) = \int_a^b K_f(t,z) y(z) dx. \tag{31}$$

Substituting equation (4) into equation (31), we obtain

$$I_n(t) = \sum_{i=0}^{n} \left[\int_a^b K_f(t,z) T_i(z) dx \right] y_i, \tag{32}$$

where the definition of $T_i(z)$ is as shown in equation (10).

Let $t = t_\theta$, $\theta = i = 0, 1, \cdots, n$; we have

$$I_n(t_\theta) = \sum_{i=0}^{n} \left[\int_a^b K_f(t_\theta, z) T_i(z) dz \right] y_i. \tag{33}$$

Equation (34) is written as follows:

$$R_{\theta i} = R_i(t_\theta) = \int_a^b K_f(t_\theta, z) T_i(z) dz. \tag{34}$$

Formula (34) is calculated by the Gauss quadrature formula with weights $\eta(z) = K_f(t_\theta, z)$; we have

$$R_{\theta i}^G = \sum_{j=1}^{m} T_i\left(z_j^\theta\right) B_j^\theta, i = 0, 1, \cdots, n, \tag{35}$$

where z_j^θ and B_j^θ are the Gauss points and Gauss weights and m is the number of the Gauss points.

Using the Gauss-Legendre quadrature formula, we obtain

$$R_{\theta i}^{\mathrm{GL}} = \frac{b-a}{2} \sum_{j=1}^{m} r\left(z_j^{\theta,l}\right) B_j^{\theta,l}, \tag{36}$$

where $z_j^{\theta,l}$ and $B_j^{\theta,l}$ are integral points and integral weights, m is the number of the integral points, $(b-a)/2$ is transformed coefficient, and $r(z_j^{\theta,l}) = \eta(z_j^{\theta,l}) T_i^{(\xi+1)}(z_j^{\theta,l})$.

Formula (33) is calculated by the Gauss quadrature formula; equation (37) is written as follows:

$$I_n(t_\theta) = \sum_{i=0}^{n} \left[R_{\theta i}^G\right] y_i. \tag{37}$$

Let $I_i = I_n(t_i)$; formula (38) is obtained

$$I = RY, \tag{38}$$

where

$$I = \begin{bmatrix} I_0 \\ \vdots \\ I_n \end{bmatrix},$$

$$Y = \begin{bmatrix} y_0 \\ \vdots \\ y_n \end{bmatrix},$$

$$R = \begin{bmatrix} R_{11} & R_{12} & \cdots & R_{1N} \\ R_{21} & R_{22} & \cdots & R_{2N} \\ \vdots & \vdots & \ddots & \vdots \\ R_{N1} & R_{N2} & \cdots & R_{NN} \end{bmatrix}_{N\times N},$$

$$N = n+1, R_{11} = \sum_{j=1}^{m} T_0\left(z_j^0\right) B_j^0,$$

$$R_{12} = \sum_{j=1}^{m} T_1\left(z_j^0\right) B_j^0, R_{1N} = \sum_{j=1}^{m} T_n\left(z_j^0\right) B_j^0,$$

$$R_{21} = \sum_{j=1}^{m} T_0\left(z_j^1\right) B_j^1, R_{22} = \sum_{j=1}^{m} T_1\left(z_j^1\right) B_j^1,$$

$$R_{2N} = \sum_{i=1}^{m} T_n\left(z_j^1\right) B_j^1, R_{N1} = \sum_{j=1}^{m} T_0\left(z_j^n\right) B_j^n,$$

$$R_{N2} = \sum_{j=1}^{m} T_1(z_i^n) B_j^n, R_{NN} = \sum_{j=1}^{m} T_n\left(z_j^n\right) B_j^n. \tag{39}$$

6. Matrix Equation for FVIDE

Equation (1) is treated by integration by parts; then, we get

$$\begin{aligned} &\Gamma_\alpha^\xi \left[\frac{\partial^\xi y(0)}{\partial t^\xi} t^{\xi-\alpha} + \int_0^t \frac{\partial^{\xi+1} y(\tau)}{\partial \tau^{\xi+1}} \frac{d\tau}{(t-\tau)^{\alpha-\xi}} \right] \\ &\quad + \int_0^t K_v(t,x) y(x) dx + \int_a^b K_f(t,z) y(z) dz = g(t). \end{aligned} \tag{40}$$

Substituting equation (4) into equation (40), equation (41) is obtained

$$\begin{aligned} &\Gamma_\alpha^\xi \left\{ \sum_{i=0}^{n} \left[T_i^{(\xi)}(0) t^{\xi-\alpha} \right] + \sum_{i=0}^{n} \left[\int_0^t \frac{T_i^{(\xi+1)}(\tau)}{(t-\tau)^{\alpha-\xi}} d\tau \right] \right\} y_i \\ &\quad + \sum_{i=0}^{n} \left[\int_0^t K_v(t,x) T_i(x) dx \right] y_i \\ &\quad + \sum_{i=0}^{n} \left[\int_a^b K_f(t,z) T_i(z) dz \right] y_i = g(t). \end{aligned} \tag{41}$$

Taking $t = t_\theta$, $\theta = 0, 1, \cdots, n$, we get

$$\begin{aligned} &\Gamma_\alpha^\xi \left\{ \sum_{i=0}^{n} \left[T_i^{(\xi)}(0) t_\theta^{\xi-\alpha} \right] + \sum_{i=0}^{n} \left[\int_0^{t_\theta} \frac{T_i^{(\xi+1)}(\tau)}{(t_\theta-\tau)^{\alpha-\xi}} d\tau \right] \right\} y_i \\ &\quad + \sum_{i=0}^{n} \left[\int_0^{t_\theta} K_v(t_\theta,x) T_i(x) dx \right] y_i \\ &\quad + \sum_{i=0}^{n} \left[\int_a^b K_f(t_\theta,z) T_i(z) dz \right] y_i = g(t_\theta). \end{aligned} \tag{42}$$

Let $g_i = g(t_i)$; combining (17), (29), and (38), we obtain the matrix equation as follows:

$$LY = G, \tag{43}$$

where

$$\begin{aligned} G &= \begin{bmatrix} g_0 \\ \vdots \\ g_n \end{bmatrix}, \\ L &= D^\alpha + Q + R. \end{aligned} \tag{44}$$

The initial conditions are imposed by replacement method and additive method. When the replacement method is used to impose initial conditions, the 1st row element of matrix I_{n+1} is extracted to replace the corresponding row element of matrix L in the system (43). When the additive method is used to impose initial conditions, the 1st row element of matrix I_{n+1} is extracted and then added to the $n+2$ row of matrix L in the system (43).

Table 1: Errors of equidistant nodes for barycentric Lagrange interpolation with $m = 6$ for Example 1.

t_i	$(n,\alpha) = (5,0.75)$	$(n,\alpha) = (10,0.75)$	$(n,\alpha) = (20,0.75)$
0	6.7117e-16	1.7418e-15	5.5914e-13
0.2	1.4468e-15	2.0154e-13	2.9617e-08
0.4	1.6376e-15	1.6798e-13	2.3200e-08
0.6	1.8041e-15	1.5907e-13	5.5773e-08
0.8	2.1094e-15	1.5510e-13	4.7605e-07
1	2.2204e-15	1.9784e-13	1.3536e-06

Table 2: Errors of equidistant nodes for barycentric rational interpolation with $m = 6$ and $d = 3$ for Example 1.

t_i	$(n,\alpha) = (5,0.75)$	$(n,\alpha) = (10,0.75)$	$(n,\alpha) = (20,0.75)$
0	2.6439e-16	4.0324e-16	1.0279e-15
0.2	1.3184e-16	1.0807e-15	2.5535e-15
0.4	6.1062e-16	1.4572e-15	2.8449e-15
0.6	8.3267e-16	1.8041e-15	3.2474e-15
0.8	9.9920e-16	2.9976e-15	1.9762e-14
1	8.8818e-16	8.8818e-16	2.4070e-13

Table 3: Errors of equidistant nodes for barycentric Lagrange interpolation using the Gauss-Legendre quadrature formula with $m = 6$ for Example 1.

t_i	$(n,\alpha) = (5,0.75)$	$(n,\alpha) = (10,0.75)$	$(n,\alpha) = (20,0.75)$
0	7.6617e-17	1.7422e-15	7.1349e-14
0.2	2.0293e-05	2.0293e-05	2.0288e-05
0.4	1.6234e-04	1.6234e-04	1.6234e-04
0.6	5.4791e-04	5.4791e-04	5.4793e-04
0.8	1.2988e-03	1.2988e-03	1.2989e-03
1	2.5366e-03	2.5366e-03	2.5369e-03

7. Numerical Experiments

In this section, several numerical examples are given to illustrate the accuracy of BICM. All of numerical examples have been performed on MATLAB (version: R2020a). The error function is defined as

$$e_n(t) = \|y_n(t) - y(t)\|, \tag{45}$$

where $y_n(t)$ and $y(t)$ are approximate solution and exact solution of numerical examples.

Example 1. Consider the linear fractional Volterra integro-differential equation with the initial condition $y(0) = 0$.

$$D^{0.75} y(t) + \frac{e^t t^2}{5} y(t) - \int_0^t e^t x y(x) dx = \frac{6t^{2.25}}{\Gamma(3.25)}, \tag{46}$$

where $0 \le t \le 1$. The analytical solution is $y(t) = t^3$.

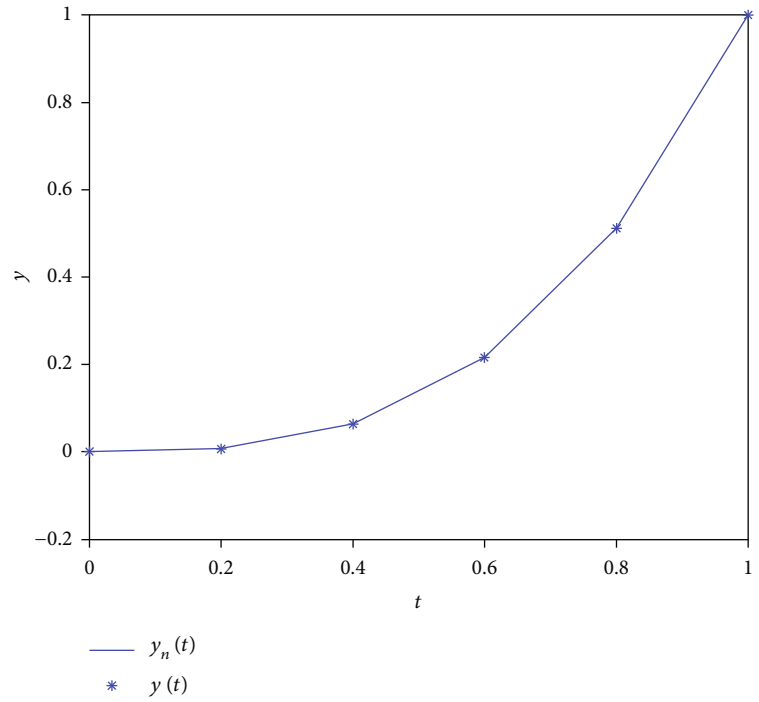

FIGURE 1: $y_n(t)$ and $y(t)$ of barycentric Lagrange interpolation using the Gauss quadrature formula with $m = 3$ at $n = 5$ for Example 1.

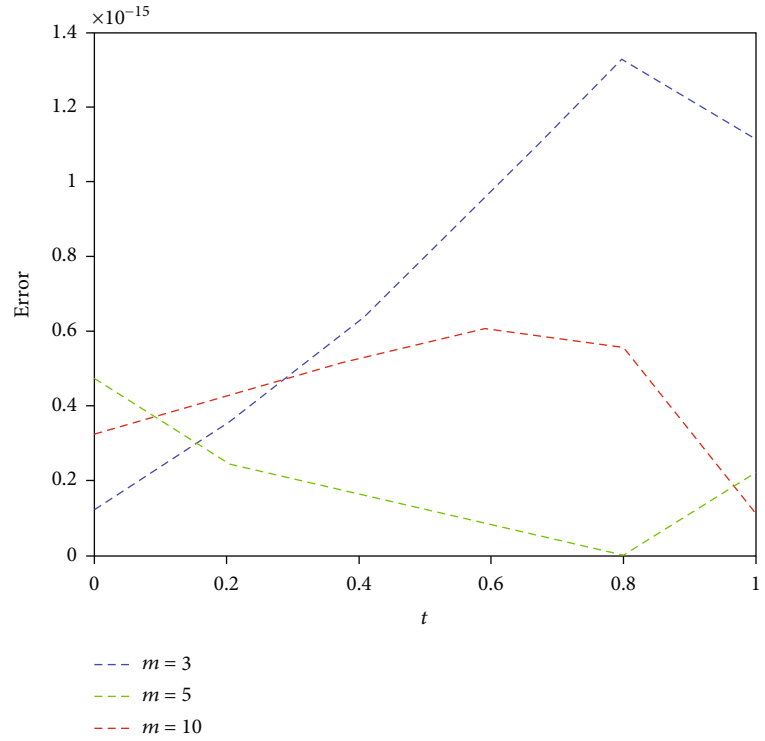

FIGURE 2: Errors of barycentric Lagrange interpolation using the Gauss quadrature formula with different Gauss points at $n = 5$ for Example 1.

In Tables 1 and 2, the errors of the Gauss quadrature formula are shown for $n = 5,10,20$ at $m = 6$. From Tables 1 and 2, we know that barycentric Lagrange interpolation and barycentric rational interpolation both get high error accuracy when $t = 0,0.2,0.4,0.6,0.8,1$. In Table 3, the errors of barycentric Lagrange interpolation with the Gauss-Legendre quadrature formula are shown. In Tables 1–3, initial conditions are imposed by replacement method. From

Table 4: Errors of equidistant nodes for barycentric Lagrange interpolation with $n = 5$ for Example 2.

t_i	$(m, \alpha) = (3,0.75)$	$(m, \alpha) = (5,0.75)$	$(m, \alpha) = (10,0.75)$
0	5.5339*e*-16	3.5112*e*-16	1.9950*e*-16
0.2	3.1745*e*-16	3.1745*e*-16	2.9317*e*-16
0.4	7.0777*e*-16	9.7145*e*-17	5.9674*e*-16
0.6	8.8818*e*-16	2.7756*e*-17	8.3267*e*-16
0.8	1.2212*e*-15	0	7.7716*e*-16
1	1.2212*e*-15	2.2204*e*-16	3.3307*e*-16

Table 5: Errors of equidistant nodes for barycentric rational interpolation with $n = 5$ and $d = 3$ for Example 2.

t_i	$(m, \alpha) = (3,0.75)$	$(m, \alpha) = (5,0.75)$	$(m, \alpha) = (10,0.75)$
0	7.8913*e*-17	3.4635*e*-16	3.4501*e*-16
0.2	3.4348*e*-16	6.1409*e*-16	6.3144*e*-16
0.4	1.3878*e*-17	4.8572*e*-16	4.5797*e*-16
0.6	1.3878*e*-16	4.1633*e*-16	5.5511*e*-16
0.8	2.2204*e*-16	3.3307*e*-16	2.2204*e*-16
1	0	1.1102*e*-15	6.6613*e*-16

Table 6: Errors of equidistant nodes for barycentric Lagrange interpolation using the additive method with $n = 5$ for Example 2.

t_i	$(m, \alpha) = (3,0.75)$	$(m, \alpha) = (5,0.75)$	$(m, \alpha) = (10,0.75)$
0	2.8897*e*-16	7.1029*e*-16	7.1941*e*-16
0.2	6.5399*e*-16	2.9317*e*-16	1.1293*e*-15
0.4	9.0206*e*-16	4.9960*e*-16	1.3600*e*-15
0.6	1.0825*e*-15	5.8287*e*-16	1.4433*e*-15
0.8	1.7764*e*-15	8.8818*e*-16	1.6653*e*-15
1	1.7764*e*-15	5.5511*e*-16	1.4433*e*-15

Tables 1 and 3, we know that error precision of barycentric Lagrange interpolation with the Gauss quadrature formula is higher than the Gauss-Legendre quadrature formula.

In Figure 1, approximate solution $y_n(t)$ and exact solution $y(t)$ are given for barycentric Lagrange interpolation using the Gauss quadrature formula with $m = 3$ at $n = 5$. Figure 2 shows errors of equidistant nodes for barycentric Lagrange interpolation using the Gauss quadrature formula with different Gauss points m. From Figures 1 and 2, we can see that higher error precision is attained when the lesser equidistant nodes are used.

Example 2. Consider the linear fractional Fredholm-Volterra integro-differential equation with the initial condition $y(0) = 1$.

$$D^{0.75}y(t) + \frac{e^t t^2}{5}y(t) - \int_0^t e^t xy(x)dx - \int_0^1 (t-x)y(x)dx = \frac{6t^{2.25}}{\Gamma(3.25)} - \frac{t}{4} + \frac{1}{5}, 0 \le t \le 1. \tag{47}$$

The analytical solution is $y(t) = t^3$.

In Tables 4–6, the errors of the Gauss quadrature formula are up to machine accuracy. In Tables 4 and 5, the initial conditions are imposed by replacement method. From Tables 4 and 6, we can find that replacement method or additive method can get high error precision.

In Figure 3, we can see that approximate solution $y_n(t)$ and exact solution $y(t)$ basically coincide. In Figure 4, errors of equidistant nodes are shown for barycentric Lagrange interpolation using the Gauss quadrature formula with different Gauss points $m = 3, 5, 10$ at $n = 5$.

Example 3. Consider the linear fractional Volterra integro-differential equation with the initial condition $y(0) = 1$.

$$D^{0.75}y(t) + ty(t) - \int_0^t txy(x)dx = \frac{t^{0.25}}{\Gamma(1.25)} - \frac{t^4}{3} - \frac{t^3}{2} - t^2 - t, 0 \le t \le 1. \tag{48}$$

The analytical solution is $y(t) = t + 1$.

Tables 7 and 8 show the errors of the Gauss quadrature formula for different m with replacement method. From these tables, BICM can obtain higher error accuracy with fewer interpolation nodes.

In Figure 5, approximate solution $y_n(t)$ and exact solution $y(t)$ are given with equidistant nodes. In Figure 6, errors of barycentric Lagrange interpolation are shown with different Gauss points m. From Figures 5 and 6, we know that

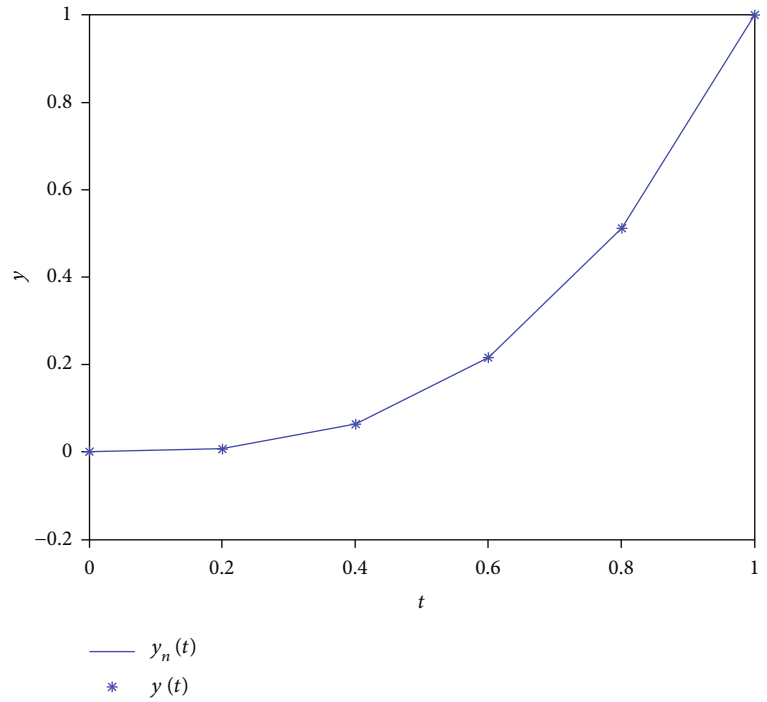

FIGURE 3: $y_n(t)$ and $y(t)$ of barycentric Lagrange interpolation using the Gauss quadrature formula with $m = 3$ at $n = 5$ for Example 2.

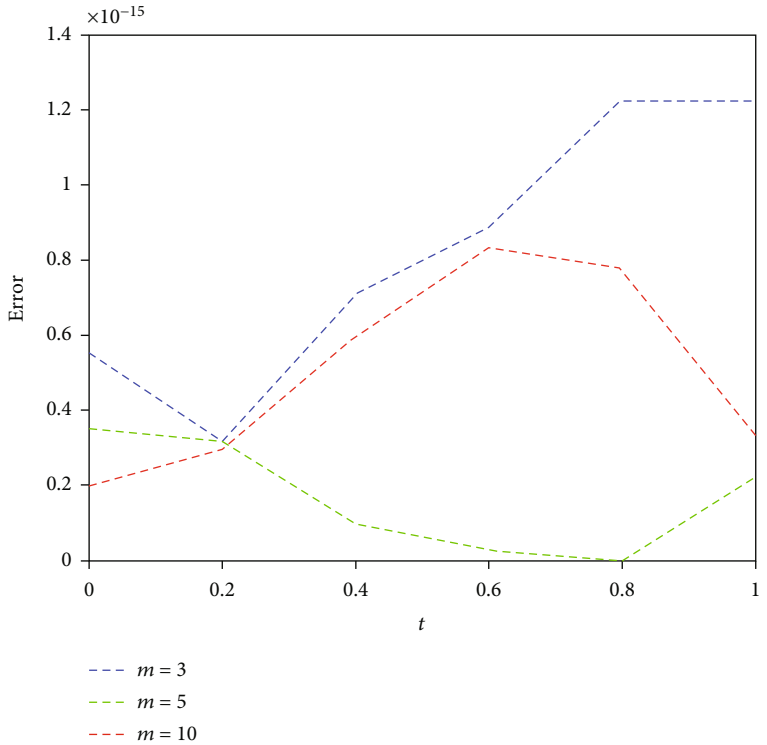

FIGURE 4: Errors of barycentric Lagrange interpolation using the Gauss quadrature formula with different Gauss points at $n = 5$ for Example 2.

Table 7: Errors of equidistant nodes for barycentric Lagrange interpolation with $n = 5$ for Example 3.

t_i	$(m, \alpha) = (3,0.75)$	$(m, \alpha) = (5,0.75)$	$(m, \alpha) = (10,0.75)$
0	8.8818*e*-16	1.3323*e*-15	1.1102*e*-16
0.2	5.5511*e*-15	4.8850*e*-15	5.1070*e*-15
0.4	5.9952*e*-15	0	2.6645*e*-15
0.6	8.8818*e*-15	8.8818*e*-16	1.1102*e*-15
0.8	1.1546*e*-14	2.2204*e*-16	3.1086*e*-15
1	1.4211*e*-14	3.9968*e*-15	1.1546*e*-14

Table 8: Errors of equidistant nodes for barycentric rational interpolation with $n = 5$ and $d = 3$ for Example 3.

t_i	$(m, \alpha) = (3,0.75)$	$(m, \alpha) = (5,0.75)$	$(m, \alpha) = (10,0.75)$
0	2.2204*e*-16	1.1102*e*-16	7.7716*e*-16
0.2	0	1.7764*e*-15	6.6613*e*-16
0.4	2.2204*e*-16	2.2204*e*-16	1.7764*e*-15
0.6	4.4409*e*-16	1.9984*e*-15	4.4409*e*-15
0.8	1.9984*e*-15	3.1086*e*-15	4.4409*e*-15
1	1.3323*e*-15	6.6613*e*-16	5.3291*e*-15

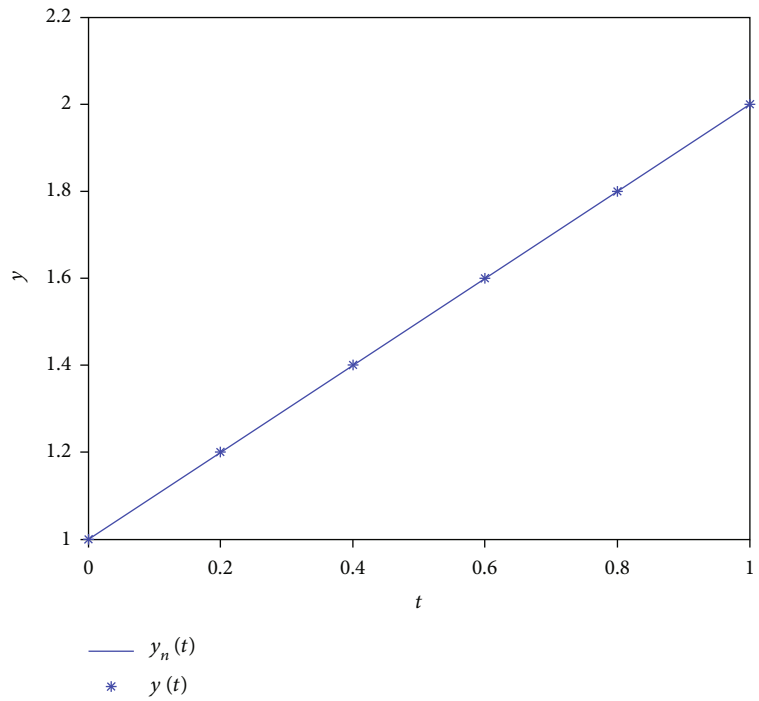

Figure 5: $y_n(t)$ and $y(t)$ of barycentric Lagrange interpolation using the Gauss quadrature formula with $m = 3$ at $n = 5$ for Example 3.

error accuracy of Barycentric Lagrange interpolation collocation method can achieve machine accuracy.

Example 4. Consider the linear fractional Volterra integrodifferential equation with the initial condition $y(0) = 0$.

$$D^{0.75}y(t) + y(t) - 2\int_0^t \sin(x-t)y(x)dx = \frac{4}{\Gamma(0.25)}\left(t^{0.25} - \int_0^t \sin(\tau)(t-\tau)^{0.25}d\tau\right) - t\cos(t), \tag{49}$$

where $0 \le t \le 1$; the analytical solution is $y(t) = \sin(t)$.

Table 9 shows the errors of the Gauss quadrature formula for the Gauss points m with barycentric Lagrange interpolation. In Table 10, taking the parameter $d = 9$ of barycentric rational interpolation, we get the errors of BICM

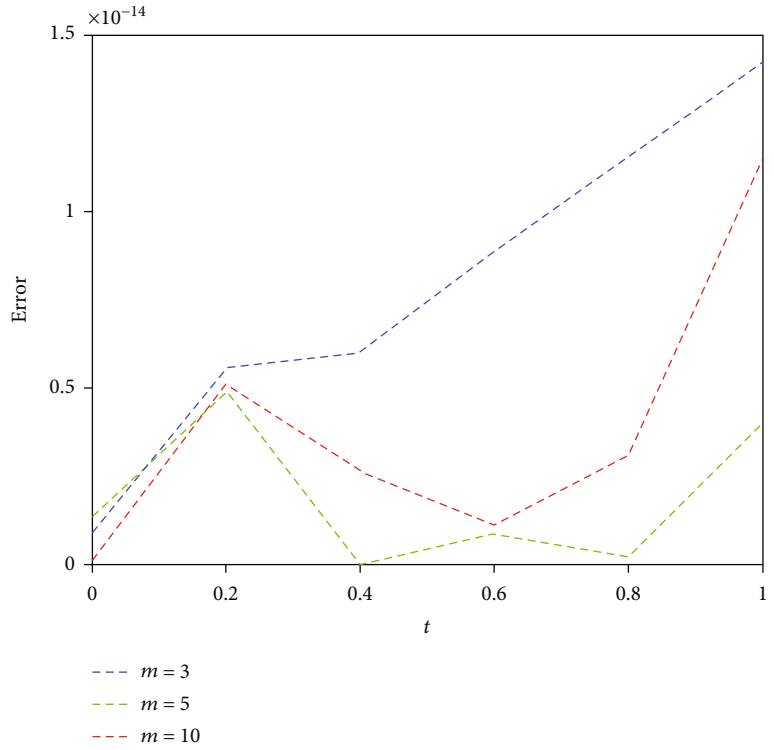

Figure 6: Errors of barycentric Lagrange interpolation using the Gauss quadrature formula with different Gauss points at $n = 5$ for Example 3.

Table 9: Errors of equidistant nodes for barycentric Lagrange interpolation with $n = 10$ for Example 4.

t_i	$(m, \alpha) = (3,0.75)$	$(m, \alpha) = (5,0.75)$	$(m, \alpha) = (10,0.75)$
0	2.7467*e*-15	1.0670*e*-14	2.3967*e*-14
0.2	5.3985*e*-13	9.6498*e*-13	1.1939*e*-12
0.4	7.5476*e*-12	1.0544*e*-12	1.3185*e*-12
0.6	2.3869*e*-10	1.1452*e*-12	1.4382*e*-12
0.8	2.7404*e*-09	1.1894*e*-12	1.4846*e*-12
1	1.7312*e*-08	1.0930*e*-12	1.4452*e*-12

Table 10: Errors of equidistant nodes for barycentric rational interpolation with $n = 10$ and $d = 9$ for Example 4.

t_i	$(m, \alpha) = (3,0.75)$	$(m, \alpha) = (5,0.75)$	$(m, \alpha) = (10,0.75)$
0	6.2870*e*-15	9.3112*e*-15	1.8457*e*-14
0.2	1.0277*e*-12	8.2812*e*-13	1.1412*e*-12
0.4	7.9721*e*-12	8.8335*e*-13	1.2341*e*-12
0.6	2.3779*e*-10	9.2648*e*-13	1.3328*e*-12
0.8	2.7337*e*-09	9.2382*e*-13	1.3728*e*-12
1	1.7293*e*-08	8.2778*e*-13	1.3872*e*-12

with equidistant nodes for different Gauss points m. Tables 9 and 10 also show the better error results.

In Figure 7, approximate solution $y_n(t)$ and exact solution $y(t)$ of the example are given at $n = 10$. In Figure 8, errors for barycentric Lagrange interpolation are shown with different Gauss points at $n = 10$. From Figures 7 and 8, barycentric Lagrange interpolation collocation method can get high error accuracy.

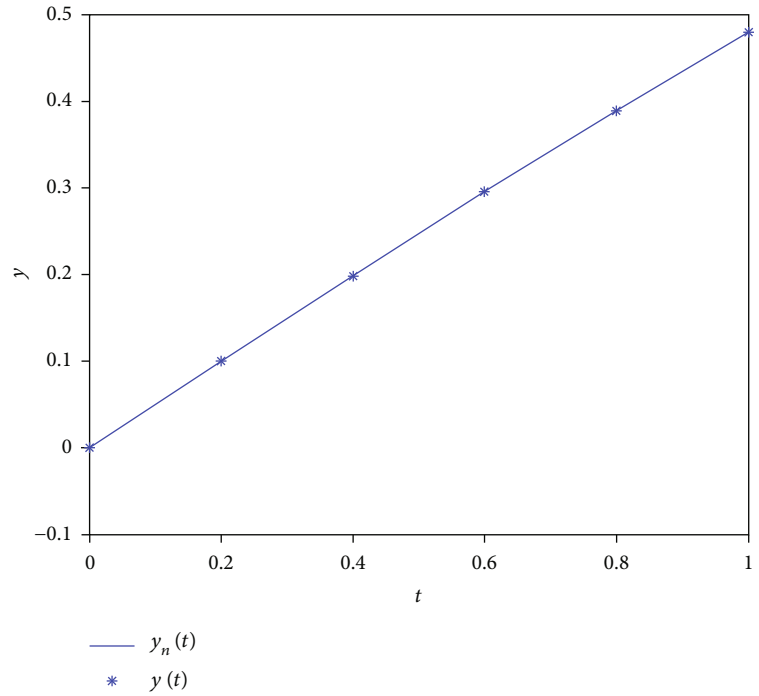

FIGURE 7: $y_n(t)$ and $y(t)$ of barycentric Lagrange interpolation using the Gauss quadrature formula with $m = 3$ at $n = 10$ for Example 4.

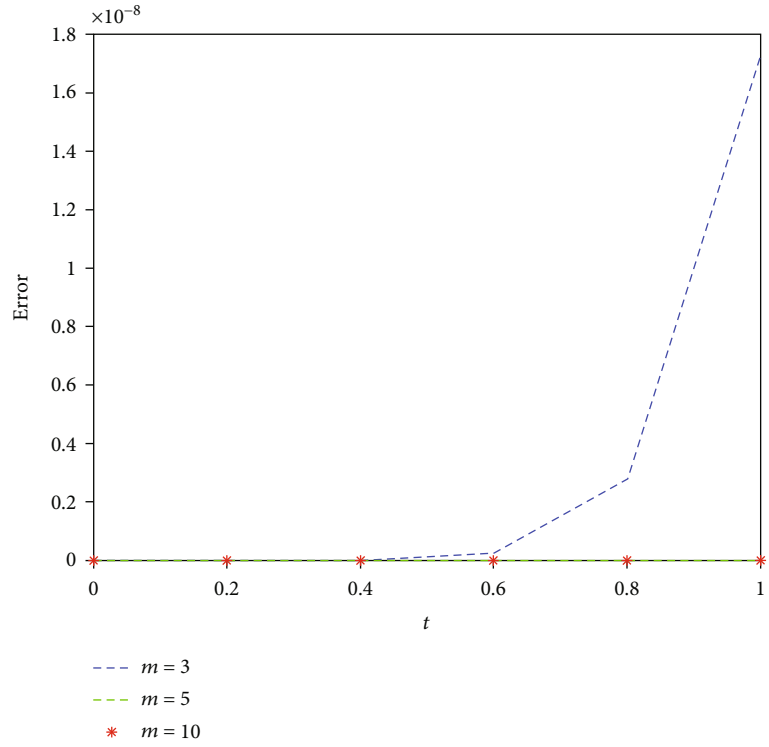

FIGURE 8: Errors of barycentric Lagrange interpolation using the Gauss quadrature formula with different Gauss points at $n = 10$ for Example 4.

8. Conclusion

BICM is proposed to solve the FVIDE. Integral terms of equation are dealt with by the Gauss quadrature formula or Gauss-Legendre quadrature formula. Compared with the Gauss-Legendre quadrature formula, barycentric Lagrange interpolation with the Gauss quadrature formula obtains higher error accuracy. The high-precise error results are gained when replacement method or additive method is chosen to deal with initial conditions. The errors of BICM are displayed by numerical examples, which illustrate that the method is available for solving one-dimensional FVIDE equation.

Data Availability

The table data and graph data used to support the findings of this study are included within the article.

Conflicts of Interest

The authors declare that they have no conflicts of interest.

Acknowledgments

The work of Jin Li was supported by the National Natural Science Foundation of China (Grant No. 11771398) and Natural Science Foundation of Hebei Province (Grant No. A2019209533).

References

[1] F. Gómez, J. Bernal, J. Rosales, and T. Cordova, "Modeling and simulation of equivalent circuits in description of biological systems-a fractional calculus approach," *Journal of Electrical Bioimpedance*, vol. 3, no. 1, pp. 2–11, 2012.

[2] B. Ghanbari, H. Günerhan, and H. M. Srivastava, "An application of the Atangana-Baleanu fractional derivative in mathematical biology: a three-species predator-prey model," *Solitons & Fractals*, vol. 138, article 109910, 2020.

[3] E. Bas and R. Ozarslan, "Real world applications of fractional models by Atangana-Baleanu fractional derivative," *Solitons & Fractals*, vol. 116, pp. 121–125, 2018.

[4] F. Jiménez and S. Ober-Blöbaum, "Fractional damping through restricted calculus of variations," *Journal of Nonlinear Science*, vol. 31, no. 2, pp. 1–43, 2021.

[5] M. V. Shitikova, "The fractional derivative expansion method in nonlinear dynamic analysis of structures," *Nonlinear Dynamics*, vol. 99, no. 1, pp. 109–122, 2020.

[6] D. Baleanu, A. Jajarmi, J. H. Asad, and T. Blaszczyk, "The motion of a bead sliding on a wire in fractional sense," *Acta Physica Polonica A*, vol. 131, no. 6, pp. 1561–1564, 2017.

[7] D. Baleanu, M. Inc, A. Yusuf, and A. I. Aliyu, "Time fractional third-order evolution equation: symmetry analysis, explicit solutions, and conservation laws," *Journal of Computational and Nonlinear Dynamics*, vol. 13, no. 2, 2018.

[8] M. Inc, A. Yusuf, A. I. Aliyu, and D. Baleanu, "Lie symmetry analysis and explicit solutions for the time fractional generalized Burgers-Huxley equation," *Optical and Quantum Electronics*, vol. 50, no. 2, pp. 1–16, 2018.

[9] J. Cao, Y. Chen, Y. Wang, G. Cheng, T. Barrière, and L. Wang, "Numerical analysis of fractional viscoelastic column based on shifted Chebyshev wavelet function," *Applied Mathematical Modelling*, vol. 91, pp. 374–389, 2021.

[10] L. Sun, Y. Chen, R. Dang, G. Cheng, and J. Xie, "Shifted Legendre polynomials algorithm used for the numerical analysis of viscoelastic plate with a fractional order model," *Mathematics and Computers in Simulation*, vol. 193, pp. 190–203, 2022.

[11] F. Gao, "General fractional calculus in non-singular power-law kernel applied to model anomalous diffusion phenomena in heat transfer problems," *Thermal Science*, vol. 21, suppl. 1, pp. 11–18, 2017.

[12] S. Krim, A. Salim, and M. Benchohra, "On implicit Caputo tempered fractional boundary value problems with delay," *Journal of Natural Sciences and Technologies*, vol. 1, no. 1, pp. 12–29, 2023.

[13] H. Afshari, V. Roomi, and M. Nosrati, "Existence and uniqueness for a fractional differential equation involving Atangana-Baleanu derivative by using a new contraction," *Progress in Fractional Differentiation and Applications*, vol. 1, no. 2, pp. 52–56, 2023.

[14] D. B. Pachpatte and J. J. Nieto, "Properties of certain Volterra type ABC fractional integral equations," *Advances in the Theory of Nonlinear Analysis and its Application*, vol. 6, no. 3, pp. 339–346, 2022.

[15] S. Abbas, M. Benchohra, J. Henderson, and J. E. Lazreg, "Weak solutions for a coupled system of partial Pettis Hadamard fractional integral equations," *Advances in the Theory of Nonlinear Analysis and its Application*, vol. 1, no. 2, pp. 136–146, 2017.

[16] R. S. Adiguzel, U. Aksoy, E. Karapinar, and I. M. Erhan, "On the solutions of fractional differential equations via Geraghty type hybrid contractions," *Applied and Computational Mathematics*, vol. 20, no. 2, pp. 313–333, 2021.

[17] R. S. Adiguzel, U. Aksoy, E. Karapinar, and I. M. Erhan, "On the solution of a boundary value problem associated with a fractional differential equation," *Mathematical Methods in the Applied Sciences*, 2020.

[18] R. S. Adiguzel, U. Aksoy, E. Karapinar, and I. M. Erhan, "Uniqueness of solution for higher-order nonlinear fractional differential equations with multi-point and integral boundary conditions," *RACSAM*, vol. 115, no. 3, p. 155, 2021.

[19] D. C. Labora, J. J. Nieto, and R. Rodríguez-López, "Is it possible to construct a fractional derivative such that the index law holds," *Progress in Fractional Differentiation and Applications*, vol. 4, no. 1, pp. 1–3, 2018.

[20] A. A. Tateishi, H. V. Ribeiro, and E. K. Lenzi, "The role of fractional time-derivative operators on anomalous diffusion," *Frontiers of Physics*, vol. 5, p. 52, 2017.

[21] M. Caputo and M. Fabrizio, "On the notion of fractional derivative and applications to the hysteresis phenomena," *Meccanica*, vol. 52, no. 13, pp. 3043–3052, 2017.

[22] J.-D. Djida, G. Mophou, and I. Area, "Optimal control of diffusion equation with fractional time derivative with nonlocal and nonsingular Mittag-Leffler kernel," *Journal of Optimization Theory and Applications*, vol. 182, no. 2, pp. 540–557, 2019.

[23] I. Podlubny, "Fractional differential equations," *Mathematics in Science and Engineering*, vol. 198, 1999.

[24] J. Losada, J. J. Nieto, and S. Arabia, "Properties of a new fractional derivative without singular kernel," *Progress in Fractional Differentiation and Applications*, vol. 1, no. 2, pp. 87–92, 2015.

[25] A. Atangana and D. Baleanu, "New fractional derivatives with nonlocal and non-singular kernel: theory and application to

heat transfer model," *Applied Mechanics and Materials*, vol. 20, no. 2, pp. 763–769, 2016.

[26] M. Caputo and M. Fabrizio, "A new definition of fractional derivative without singular kernel," *Progress in Fractional Differentiation and Applications*, vol. 1, no. 2, pp. 73–85, 2015.

[27] S. G. Samko, A. A. Kilbas, and O. I. Marichev, "Fractional integrals and derivatives: Theory and applications," *Gordon and Breach*, vol. 1, 1993.

[28] S. Shamseldeen, A. Elsaid, and S. Madkour, "Caputo-Riesz-Feller fractional wave equation: analytic and approximate solutions and their continuation," *Journal of Applied Mathematics and Computing*, vol. 59, no. 1–2, pp. 423–444, 2019.

[29] Ş. Yüzbaşı, "Fractional Bell collocation method for solving linear fractional integro-differential equations," *Mathematical Sciences*, 2022.

[30] E. Sousa, "Numerical approximations for fractional diffusion equations via splines," *Computers & Mathematics with Applications*, vol. 62, no. 3, pp. 938–944, 2011.

[31] V. J. Ervin and J. P. Roop, "Variational formulation for the stationary fractional advection dispersion equation," *Numerical Methods for Partial Differential Equations: An International Journal*, vol. 22, no. 3, pp. 558–576, 2006.

[32] V. J. Ervin and J. P. Roop, "Variational solution of fractional advection dispersion equations on bounded domains in $\mathbb{R}^d$," *Numerical Methods for Partial Differential Equations*, vol. 23, no. 2, pp. 256–281, 2007.

[33] M. Abbaszadeh and M. Dehghan, "A meshless numerical procedure for solving fractional reaction subdiffusion model via a new combination of alternating direction implicit (ADI) approach and interpolating element free Galerkin (EFG) method," *Computers & Mathematics with Applications*, vol. 70, no. 10, pp. 2493–2512, 2015.

[34] M. Dehghan and M. Abbaszadeh, "Analysis of the element free Galerkin (EFG) method for solving fractional cable equation with Dirichlet boundary condition," *Applied Numerical Mathematics*, vol. 109, pp. 208–234, 2016.

[35] M. Dehghan, M. Abbaszadeh, and A. Mohebbi, "Error estimate for the numerical solution of fractional reaction-subdiffusion process based on a meshless method," *Journal of Computational and Applied Mathematics*, vol. 280, pp. 14–36, 2015.

[36] J. Li and Y. L. Cheng, "Linear barycentric rational collocation method for solving heat conduction equation," *Numerical Methods for Partial Differential Equations*, vol. 37, no. 1, pp. 533–545, 2021.

[37] J. Li, Y. L. Cheng, Z. C. Li, and Z. K. Tian, "Linear barycentric rational collocation method for solving generalized Poisson equations," *Mathematical Biosciences and Engineering*, vol. 20, no. 3, pp. 4782–4797, 2023.

[38] J. Li, X. N. Su, and K. Y. Zhao, "Barycentric interpolation collocation algorithm to solve fractional differential equations," *Mathematics and Computers in Simulation*, vol. 205, pp. 340–367, 2023.

[39] J. Li, "Barycentric rational collocation method for fractional reaction-diffusion equation," *AIMS Mathematics*, vol. 8, no. 4, pp. 9009–9026, 2023.

[40] M. Zhuang, C. Miao, and S. Ji, "Plane elasticity problems by barycentric rational interpolation collocation method and a regular domain method," *International Journal for Numerical Methods in Engineering*, vol. 121, no. 18, pp. 4134–4156, 2020.

[41] Z. Q. Wang, J. Jiang, and B. T. Tang, "Numerical solution of bending problem for elliptical plate using differentiation matrix method based on barycentric Lagrange interpolation," *Applied Mechanics and Materials*, vol. 638, pp. 1720–1724, 2014.

[42] Z. Q. Wang, B. T. Tang, and W. Zheng, "A Barycentric interpolation collocation method for Darcy flow in two-dimension," *Applied Mechanics and Materials*, vol. 684, pp. 3–10, 2014.